International Journal of Latest Research in Engineering and Technology (IJLRET)
ISSN: 2454-5031(Online)
www.ijlret.com ‖ Volume 1 Issue 1 ‖ June 2015 ‖ PP.01-09

A two-switch multi-input step-up DC/DC converter for PV systems

Mahdi Elmi[1], Mohamad Reza Banaei[2]
[1] *Department of Electrical Engineering, Azarbaijan Shahid Madani University, Tabriz, Iran*
[2] *Department of Electrical Engineering, Azarbaijan Shahid Madani University, Tabriz, Iran*

Abstract— This study presents a new two-switch multi-input high step-up DC/DC converter. A coupled inductor is used to enhance the voltage gain. Having a bidirectional port makes the converter suitable for applications in need of battery such as stand-alone photovoltaic (PV) systems. As a result, the proposed converter has the merits of integrating two power sources along with boosting the input voltage. Furthermore, in comparison with typical three-port DC/DC converters which utilize three switches, the presented converter employ only two switches to control the converter. Hence, cost and size of the structure is reduced. In order to verify the performance of the converter, simulation results are taken and depicted.
Keywords— multi-input, DC/DC converter, high step-up, stand-alone PV systems, maximum power point tracking (MPPT) algorithm.

I. INTRODUCTION

Currently, a great proportion of electricity used around the world is generated by burning fossil fuels such as gas and coal. This makes the electricity sector one of the biggest contributors to greenhouse emissions. On the other hand, the sources of fossil fuels are limited and going to be used up completely in near future. Aforementioned problems along with capability of renewable energy resources in generating electricity have lead the governments and researchers to increase the contribution of them in electric production. Among these resources, PV systems have noticeable features including noiseless function, no pollution, vast scale availability and low maintenance cost [1]. However, intermittent feature of PVs is one of their main drawbacks. Hence, PV systems are accompanied with an energy storage system (ESS) to balance the power between PV modules and load in stand-alone renewable power system applications [2]. One feature that must be taken into account in designing the interface converter for PV systems is the bidirectional power flow capability of storage element port. In conventional systems, multiple individual converters have been used for each power supply (either unidirectional or bidirectional). Nowadays, compared to typical structures, multi-input converters (MICs) offer a compact converter with centralized control, higher reliability and efficacy, lower size and cost reduction [3]. In recent literature, a number of works have been reported in designing a compact converter which could integrate two power supplies to the utility grid or load [4-5]. A compact three port DC-DC converter is studied in [4]. One of the merits of the presented converter is having a bidirectional port which makes it suitable for applications in need of battery. Moreover, the number of utilized elements is reduced in comparison with conventional structures. However, low voltage ratio of the converter makes it unsuitable in high voltage gain applications. In [5], an isolated three-phase high step-up DC-DC converter is used for integrating renewable energy resources into the grid or load. By the use of three-phase high frequency transformer, high voltage gain is achieved. The converter utilizes only three switches which results in a higher efficiency. However, another converter is needed to connect the battery to the DC bus. A compact two-input converter is proposed for standalone PV systems in [6]. Moreover, high voltage gain of the converter makes the converter suitable for low input voltage applications. However, the high number of semiconductors and passive elements reduce the efficiency.

This paper presents a novel two-switch high step-up multi-port DC-DC converter to integrate stand-alone PV system and battery unit into the DC bus. Compared to conventional multi-ports which use at least three switches to hybridize a power source and a battery, the proposed converter has only two switches. Hence, cost and size of the converter is significantly reduced. Meanwhile, high step-up capability of the converter makes it a promising converter for power supplies with low output voltage, such as PVs. Performance of the converter in three states including no battery, battery charging and battery discharging is analyzed. The rest of the paper is devoted as followings. In the next section, analysis of the converter is given. Employed power management method is described in Section III. In section IV, simulation results are depicted. Finally, section V concludes the whole paper.

II. OPERATION PRINCIPLES

A) Circuit Principles

The structure of proposed converter is shown in Fig. 1. The circuit consists of two power switches, five diodes, three capacitors and one coupled inductor. Vi is the primary input and battery is assumed as second input. Coupled inductor is modeled as magnetize inductor Lm, leakage inductor Lk and an ideal transformer N_2/N_1. In order to simplify the circuit analysis, following assumptions are taken:

1) The proposed converter is analyzed in continuous conduction mode (CCM).
2) Capacitors C_1, C_2 and C_o are large enough and voltage across them are considered as constant voltages.
3) Turn ratio of transformer N_2/N_1 is assumed as n.
4) The power switches and diodes are ideal.
5) The coupling coefficient of the couple inductor k equals to Lm/(Lm+Lk).

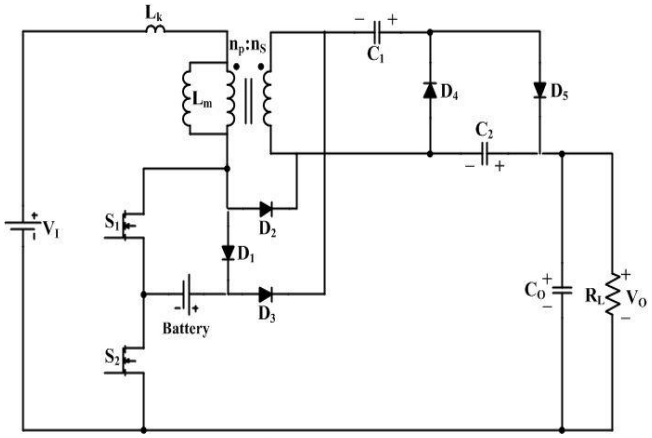

Fig. 1. *Proposed Converter's Circuit Structure*

B) Operation States

The proposed converter can operate in three different states which are described in followings:

1) Single input: Main power source supplies the load and battery is not connected.
2) Battery charging: Main power source supplies the load and battery is charged.
3) Battery discharging: Main power source supplies the load and battery is discharged.

First State (Single input): In this state, V_i furnishes the load without the battery. This state consists of five operation modes (Fig. 2.).

Operation mode I [t_0-t_1]: This operation mode begins at t_0 by turning switches S_1 and S_2 on. Diode D_4 conducts and other four diodes are off. The load is supplied by output capacitor C_o and input source charges the coupled inductor. This mode ends when the current of secondary windings of coupled inductor reaches zero.

Operation mode II [t_1-t_2]: This operation mode begins at t_1, when diode D4 turns off with ZCS. During this state, current of leakage inductor is bigger than current of magnetizing inductor. Diode D5 is on and others are off. The load is supplied by output capacitor C_o and input source charges the coupled inductor. This mode ends when switches S_1 and S_2 are turned off.

Operation mode III [t_2-t_3]: By turning switches S_1 and S_2 off, diode D_2 will be turned on. Since the currents of primary and secondary sides of coupled inductor is not equal, clamp diode D_2 conducts and the stored energy in leakage inductor is transmitted to the output load. During this mode, diode D_5 conducts and diodes D_1, D_3 and D_4 remain off. This mode ends when the current of secondary windings reaches zero.

Operation mode IV [t_3-t_4]: in this mode, switches S_1 and S_2 are off and diodes D_1, D_2 and D_3 conduct. Diodes D_4 and D_5 are off. During this mode stored energy in capacitor C2 is transmitted to the output. This mode ends when switch $S_1$is turned on.

Operation mode V [t_4-t_5]: This mode begins when diode D_2 turns off with ZCS and continues until switches S_1 and S_2 are turned on. Diodes D_1, D_2 and D_4 are off. During this mode energy of input source, coupled inductor and capacitor C_2 is transmitted to the output load and capacitor.

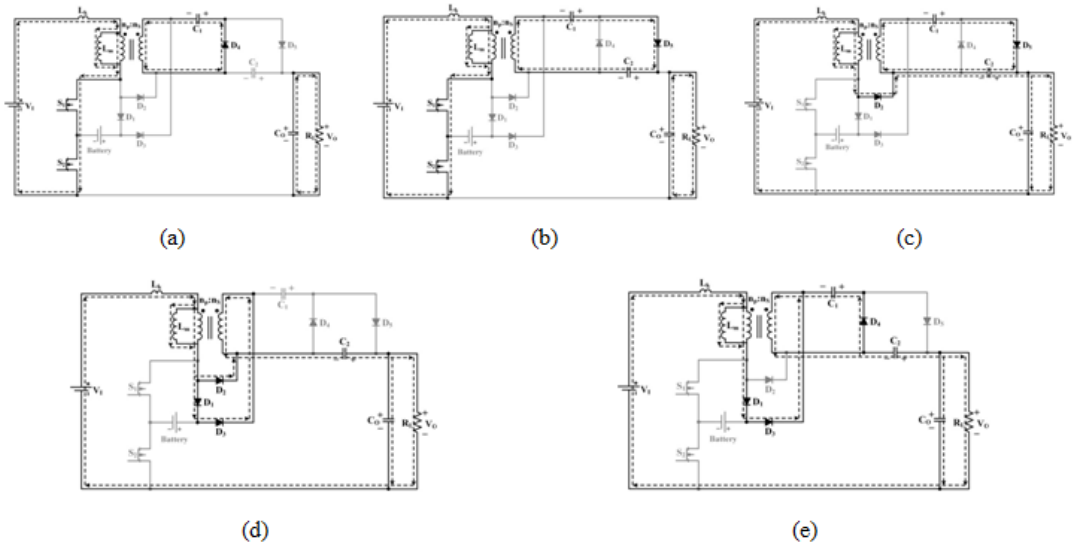

Fig. 2. Operation states of first state. (a) [t_0-t_1], (b) [t_1-t_2], (c) [t_3-t_4], (d) [t_4-t_5] and (e) [t_5-t_6]

Typical waveforms of first state are depicted in Fig.3.

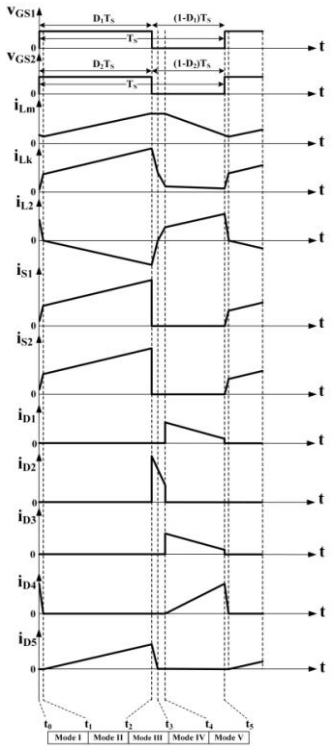

Fig. 3.*Wave forms of first state*

Second State (Battery charging): In this state, main power source supplies the load and charges the battery. This state consists of six operation modes (Fig. 4.).

Operation mode I [t_0-t_1]: This mode begins by turning switch S_2 on. During this mode, diodes D_1 and D_4 are on and diodes D_2, D_3 and D_5 are off. Meanwhile, input source charges the battery and output capacitor C_O charges the load. Secondary side of coupled inductor charges capacitor C_1. This mode ends when current of secondary side of coupled inductor reaches zero.

Operation mode II [t_1-t_2]: This mode begins when diode D_4 turns off with ZCS. In this mode the currents of L_k and L_m are equal and coupled inductor is charged. During this mode switch S_2 and diode D_1 are on and switch S1 and diodes D_2, D_3, D_4 and D_5 are off. This mode ends by turning S_1 on.

Operation mode III [t_2-t_3]: This mode begins at t_3 by turning switch S_1 on. Diodes D_1, D_2, D_3 and D_4 are off. Input source charges the coupled inductor and output capacitor C_O charges the load. Diode D_5 conducts and capacitors C_1 and C_2 are charged by the secondary side of coupled inductor.

Operation mode IV [t_3-t_4]: By turning switches S_1 and S_2 off, diode D_2 will be turned on. Since the currents of primary and secondary sides of coupled inductor is not equal, clamp diode D_2 conducts and the stored energy in

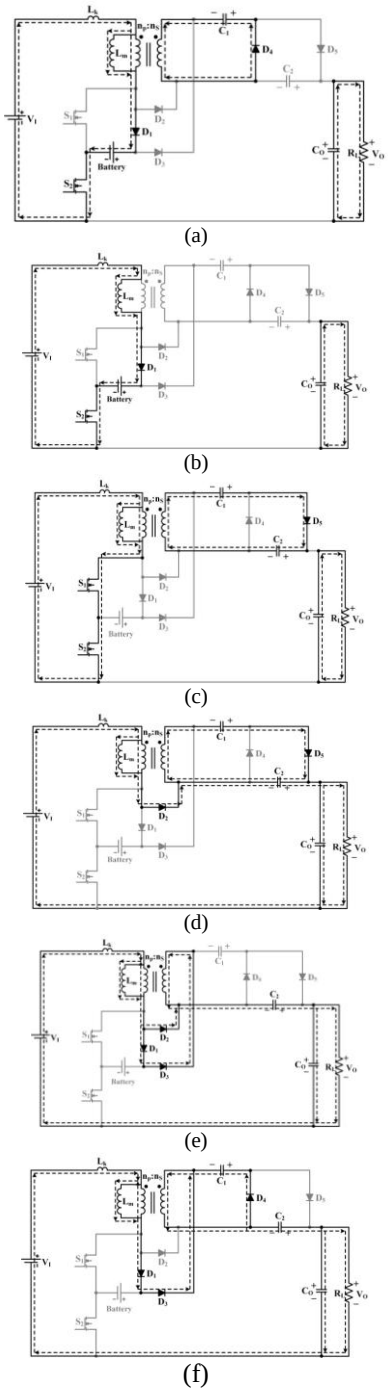

Fig. 4 Operation modes of second state. (a) [t_0-t_1], (b) [t_1-t_2], (c) [t_2-t_3], (d) [t_3-t_4], (e) [t_4-t_5] and (f) [t_5-t_6]

leakage inductor is transmitted to the output load. During this mode, diode D_5 conducts and diodes D_1, D_3 and D_4 remain off. This mode ends when the current of secondary windings reaches zero.

Operation mode V [t_4-t_5]: in this mode, switches S_1 and S_2 are off and diodes D_1, D_2 and D_3 conduct. Diodes D_4 and D_5 are off. During this mode stored energy in capacitor C2 is transmitted to the output. This mode ends when switch $S_1$is turned on.

Operation mode VI [t_5-t_6]: This mode begins when diode D_2 turns off with ZCS and continues until switches S_1 and S_2 are turned on. Diodes D_1, D_2 and D_4 are off. During this mode energy of input source, coupled inductor and capacitor C_2 is transmitted to the output load and capacitor. Operation wave forms of second state are depicted in Fig. 6.

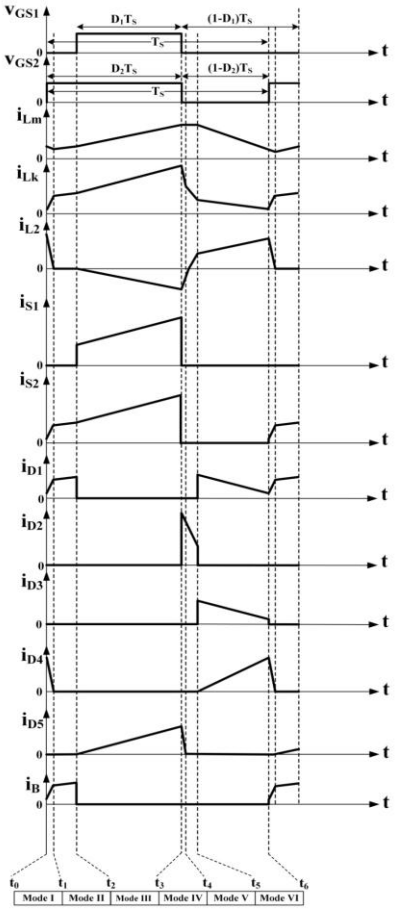

Fig. 5. Wave forms of second state

Third State (battery discharging): In this state, main power source and the battery supply the load and the battery is being discharged. This state consists of seven operation modes (Fig. 6.).

Operation mode I [t_0-t_1]: First mode begins by turning switch S_1 on. Diodes D_3 and D_4 are on and diodes D_1, D_2 and D_5 are off. During this mode, stored energy in the battery, energy of input source, coupled inductor and capacitor C_2 are transmitted to the output load and V capacitor.

Operation mode II [t_1-t_2]: Second operation mode begins when diode D4 turns off with ZCS. During this mode current of magnetizing inductor is bigger than the current of leakage inductor. During this mode switch S1 and diode D3 are on and switch S2 and diodes D1, D2, D4 and D5 are off. Meanwhile energy of input source, the battery, coupled inductor and capacitor C2 is transmitted to the output load and capacitor.

Operation mode III [t_2-t_3]: Third operation mode starts when switch S_1 and S2 are turned on. During this mode diode D4 is still on and the other diodes are off. In this mode, input power source charge the coupled inductor. And output capacitor Co charges the load. Secondary side of coupled inductor charges the capacitor C_1.

Operation mode I [t3-t4]: This mode begins when diode D_4 turns off with ZCS. During this mode, both switches are on and diodes D1, D2, D3 and D4 are off. Meanwhile, the current of leakage inductor is bigger than magnetizing inductor and the current flowing through the secondary side of the coupled inductor is negative.

Operation mode V [t_4-t_5]: By turning switches S_1 and S_2 off, diode D_2 will be turned on. Since the currents of primary and secondary sides of coupled inductor is not equal, clamp diode D_2 conducts and the stored energy in

leakage inductor is transmitted to the output load. During this mode, diode D_5 conducts and diodes D_1, D_3 and D_4 remain off. This mode ends when the current of secondary windings reaches zero.

Operation mode VI [t_5-t_6]: in this mode, switches S_1 and S_2 are off and diodes D_1, D_2 and D_3 conduct. Diodes D_4 and D_5 are off. During this mode stored energy in capacitor C2 is transmitted to the output. This mode ends when switch $S_1$is turned on.

Operation mode VII [t_6-t_7]: This mode begins when diode D_2 turns off with ZCS and continues until switches S_1 and S_2 are turned on. Diodes D_1, D_2 and D_4 are off. During this mode energy of input source, coupled inductor and capacitor C_2 is transmitted to the output load and capacitor.

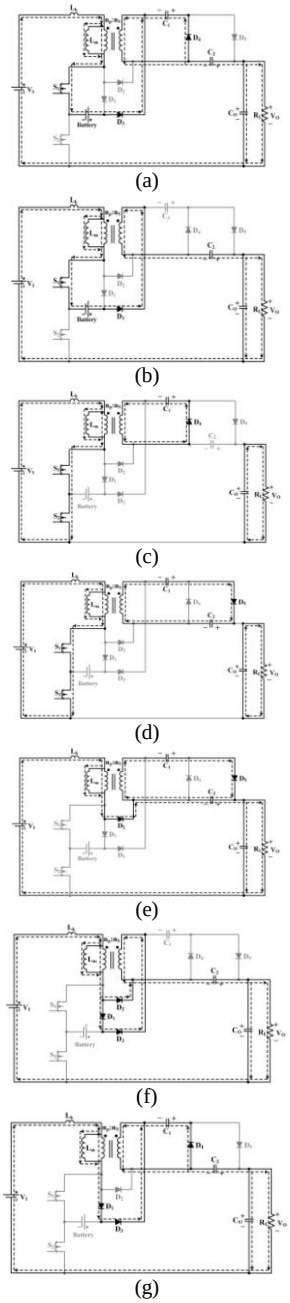

Fig. 6 Operation states twos' modes. (a) [t_0-t_1], (b) [t_1-t_2], (c) [t_2-t_3], (d) [t_3-t_4], (e) [t_4-t_5], (f) [t_5-t_6] and (g) [t_6-t_7]

Operation wave forms of third state are depicted in Fig. 7.

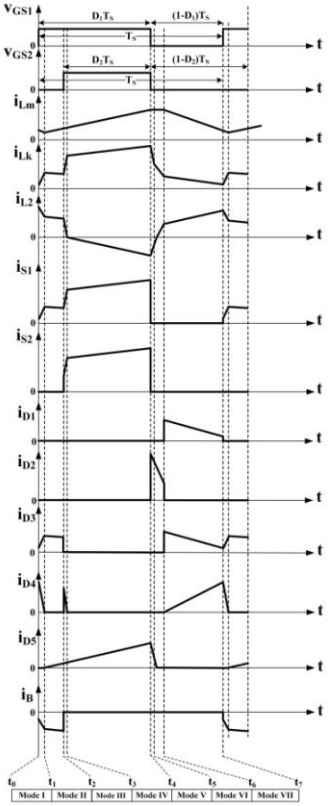

Fig. 7 Wave forms of third state

C) **Steady-state Analysis of Proposed Converter**

In order to simplify the analysis of the converter, in addition to assumptions made in pervious section, the followings are also made:

- Leakage inductance of coupled inductor L_k is ignored.
- D_{s1} and D_{s2} represent the duty ratios of switches S_1 and S_2, respectively.

A. First state (Single input)

Voltage gain of the converter in first state can be calculated as follows:

$$M_{V\,DC} = \frac{1+n+nD}{1-D} \tag{1}$$

B. Second state(Battery charging)

Using the same procedure for this state, output voltage of the converter in second state can be calculated as follows:

$$V_O = \frac{(1+n+nD_{S2})V_{in} - (2n+1)(D_{S2} - D_{S1})V_B}{1-D_{S2}} \tag{2}$$

C. Third state(Battery discharging)

Likewise, output voltage of the converter in third state can be calculated as follows:

$$V_O = \frac{(1+n+nD_{S1})V_{in} + \frac{(2n+1)}{n}(D_{S1} - D_{S2})V_B}{1-D_{S1}} \tag{3}$$

III. MAXIMUM POWER POINT TRACKING (MPPT) METHOD

The other main disadvantage of PV systems is that the efficiency of energy conversion is low at present. In order to enhance the overall efficiency of system and reduce the cost of energy, it is important to make the PV system work in MPP. In literature, different procedures have been addressed by researchers to achieve MPPT [7-9]. Static optimization algorithms such as Perturb and observe (P&O) algorithm [7], incremental conductance algorithm [8] and ripple correlation control (RCC) algorithm [9] have been discussed and presented in recent

researches. Simple programming and implementation, and low computation have made the P&O method a practical and widely used scheme among other schemes. However, MPPT methods based on static optimization have slower convergence in comparison with dynamic MPPT controls.

IV. SIMULATION RESULTS

The proposed system is investigated in MATLAB/SIMULINK. The specifications of the circuit are given in Tables I.

TABLE I

SPECIFICATIONS OF THE PROPOSED CONVERTER

Specifications	Values
Input voltage (V_{in})	40 V
Battery voltage (V_B)	12 V
Output voltage (V_{out})	1st state:305 V 2nd state:290 V 3rd state:315 V
Switching frequency (f_s)	50 kHz
Coupled inductor	L_K: 1 µH, L_m: 200 µH N_S/N_P=2
Output capacitor (C_o)	220 µF
Load (R_L)	3.2 Ω

Output voltage in three different stages is depicted in Fig. 8. Input current and current flowing through the battery bank are illustrated in Fig. 9 and 10, respectively. All figures are divided into three parts. In first part, battery is not used. In second part, battery is charged and in the last part, battery is discharged. Fig. 10 shows the current flowing through the battery bank. In first part, it has zero value, in second and third parts, it has a positive and negative average, respectively.

V. CONCLUSION

In this paper, a new two-switch multi-input high step-up DC/DC converter was proposed and studied. The converter is suitable for domestic and industrial applications such as stand-alone PV systems, shipboard system, and hybrid electric vehicles. Analysis of the converter was given for three operational modes including no battery, battery charging, and battery discharging. Compared to the typical dual input DC/DC converters which use three switches, the presented converter utilizes only two switches. Hence the cost and size of the converter is significantly reduced. Moreover, simulation results validated the promising performance of the converter.

References

[1] Nejabatkhah, F.; Danyali, S.; Hosseini, S.H.; Sabahi, M.; Niapour, S.M., "Modeling and Control of a New Three-Input DC–DC Boost Converter for Hybrid PV/FC/Battery Power System," Power Electronics, IEEE Transactions on , vol.27, no.5, pp.2309,2324, May 2012

[2] Hongfei Wu; Runruo Chen; Junjun Zhang; Yan Xing; Haibing Hu; Hongjuan Ge, "A Family of Three-Port Half-Bridge Converters for a Stand-Alone Renewable Power System," Power Electronics, IEEE Transactions on , vol.26, no.9, pp.2697,2706, Sept. 201

[3] Danyali, S.; Hosseini, S.H.; Gharehpetian, G.B., "New Extendable Single-Stage Multi-input DC–DC/AC Boost Converter," Power Electronics, IEEE Transactions on , vol.29, no.2, pp.775,788, Feb. 2014

[4] Rong-Jong Wai; Chung-You Lin; Bo-Han Chen, "High-Efficiency DC–DC Converter With Two Input Power Sources," Power Electronics, IEEE Transactions on , vol.27, no.4, pp.1862,1875, April 2012

[5] Zhan Wang; Hui Li, "An Integrated Three-Port Bidirectional DC–DC Converter for PV Application on a DC Distribution System," Power Electronics, IEEE Transactions on , vol.28, no.10, pp.4612,4624, Oct. 2013

[6] Li-Jhan Chien; Chien-Chih Chen; Jiann-Fuh Chen; Yi-Ping Hsieh, "Novel Three-Port Converter With High-Voltage Gain," Power Electronics, IEEE Transactions on , vol.29, no.9, pp.4693,4703, Sept. 2014

[7] Roman,E., Alonso,R., Ibanez,P.,Elorduizapatarietxe,S., and Goitia,D.: 'Intelligent PV module for grid-connected PV systems',IEEE Trans. Ind. Electron., vol. 53, no. 4, pp. 1066–1073 2006

[8] Kwon,J. M., Nam,K. H., and Kwon,B. H.: "Photovoltaic power conditioning system with line connection", IEEE Trans. Ind. Electron., vol. 53, no. 4, pp. 1048–1054 2006

[9] S. L. Brunton, C. W. Rowley, S. R.Kulkarni, and C. Clarkson, "Maximum power point tracking for photovoltaic optimization using ripple-based extremum seeking control," IEEE Trans. Power Electron., vol. 25, no. 10,pp. 2531–2540, Oct. 2010.

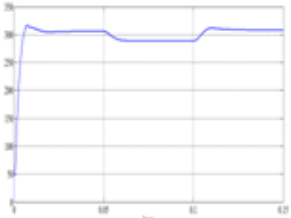

Fig. 8. Output voltage

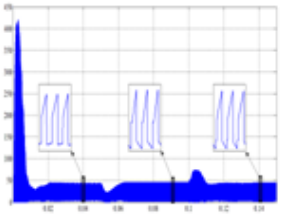

Fig. 9. Input current

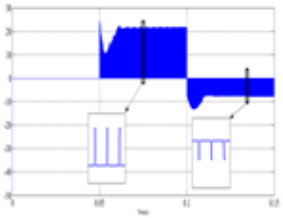

Fig. 10. Battery current